

Supporting Information: Two-stage melting induced by dislocations and grain boundaries in Monolayers of Hard Spheres

Weikai Qi,¹ Anjan P. Gantapara,¹ and Marjolein Dijkstra^{1,*}

¹*Soft Condensed Matter, Debye Institute for Nanomaterials Science, Utrecht University, Princetonplein 5, 3584 CC Utrecht, The Netherlands*

(Dated: November 5, 2013)

TWO-PHASE COEXISTENCE REGION IN COLLOIDAL MONOLAYERS

We performed large-scale event-driven Molecular Dynamics (EDMD) simulations of hard spheres with diameter σ confined between two parallel hard walls in the NVT ensemble for varying plate separations $1 \leq H/\sigma \leq 1.53$. We note that our system reduces to the 2D system of hard disks for $H/\sigma = 1$. We employed a simulation box consisting of two rectangular walls with aspect ratio $L_x : L_y = 2 : \sqrt{3}$ in order to accommodate a crystalline layer with triangular symmetry. We mention that a square simulation box was employed in the case of 2D hard disks in Refs. [1, 2], which is not commensurate with a triangular lattice and which may affect the results.

In an EDMD simulation, the system evolves via a time-ordered sequence of collision events. The spheres move at constant velocity between collisions, and the velocities of the respective particles are updated when a collision occurs. All collisions are elastic and preserve energy and momentum. In order to speed up the equilibration we divided the simulation box into small cells in the XY plane, and we used a cell list. In addition, we employed an event calendar to maintain a list of all future events [3]. Three different events are listed in the calendar: (1) collisions between particles; (2) collisions between particles with the two walls; and (3) particles that cross a cell boundary. For more details, we refer the interested reader to Ref. [3] for the implementation of the cell list and the event calendar. We performed simulations of $10^4\tau$ with $\tau = \sqrt{m/k_B T}\sigma$ the unit of time and $m = 1$ the mass of the particles.

We computed the reduced 2D lateral pressure P^* from the collision rate via the virial theorem given by $P^* = \beta P\sigma^2 = \frac{N\sigma^2}{A} \left[1 - \frac{\beta m}{2t} \frac{1}{N} \sum \mathbf{r}_{ij} \cdot \mathbf{v}_{ij} \right]$, where t denotes the time interval, and \mathbf{r}_{ij} and \mathbf{v}_{ij} are the 2D projections of the distance vector and the velocity vector, respectively, between particle i and j . In Fig. 1, we plot P^* as a function of the 2D packing fraction $\eta = \pi N\sigma^2/4A$ for $N = 128^2, 256^2, 512^2$ and 1024^2 hard spheres and $H/\sigma = 1$. We clearly observe a Mayer-Wood loop in the equation of state due to interfacial tension effects in finite systems, which becomes less pronounced for larger system sizes as expected [4].

We determine the coexisting densities using a Maxwell construction as displayed in Fig. 2, where we plot P^* as a function of the area per particle $A/N\sigma^2$. The height of the horizontal line is such that the orange areas below and above the horizontal line are equal. The interface free energy per particle is the sum of the two orange areas divided by two. From the Maxwell construction, we obtain the two-phase coexistence for $0.699 \leq \eta \leq 0.717$, which matches well with the results obtained for the 2D hard-disk system [1, 2]. In addition, we find that the interface free energy per particle f scales as $\beta f \propto N^{-1/2}$, which strongly suggests a first-order transition [1, 4].

We also calculated the coexisting densities as obtained from the Maxwell construction to the equation of state of $N = 1024^2$ hard spheres for other values of the plate separation $1 \leq H/\sigma \leq 1.53$. In Fig. 3, we plot the reduced pressure P^* as a function of the area per particle $A/N\sigma^2$ for $H/\sigma = 1.1, 1.2, 1.3, 1.4, 1.5$ and 1.53 together with the

TABLE I: The coexisting densities of the liquid and hexatic phase, η_L and η_H , respectively, the interface free energy per particle f as obtained from the Maxwell construction, and the density η_{HS} of the hexatic-solid transition determined by the finite size scaling analysis.

H/σ	η_L	η_H	f (10^{-4})	η_{HS}
1.0	0.699	0.717	0.710	0.725
1.1	0.700	0.718	1.208	0.728
1.2	0.705	0.723	1.078	0.734
1.3	0.713	0.730	1.056	0.740
1.4	0.728	0.747	1.272	0.756
1.45	0.744	0.760	1.916	0.768
1.5	0.768	0.783	2.872	0.790
1.53	0.794	0.807	3.552	0.808

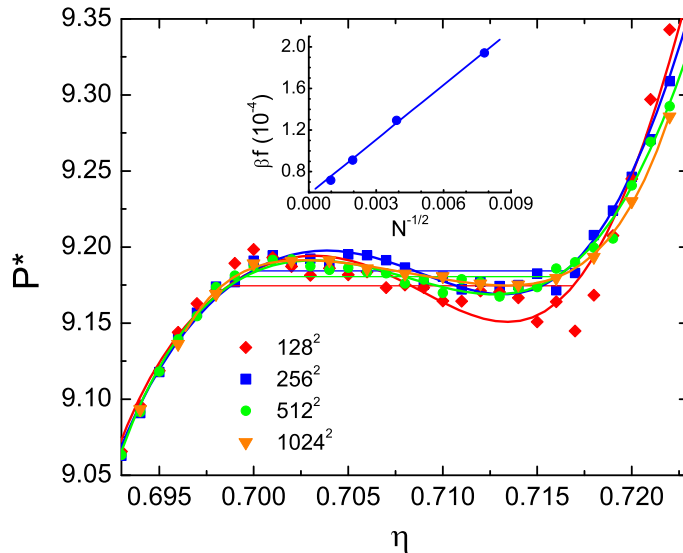


FIG. 1: The reduced 2D lateral pressure $P^* = \beta P \sigma^2$ as a function of the 2D packing fraction $\eta = \pi N \sigma^2 / 4A$ for $N = 128^2$ (red), $N = 256^2$ (blue), $N = 512^2$ (green) and $N = 1024^2$ (orange) hard spheres confined between two parallel hard walls with plate separation $H/\sigma = 1$. The symbols are simulation data and the lines are 7th-order polynomial fits. The horizontal lines indicate the coexistence regions as obtained from the Maxwell construction. The inset shows the interface free energy per particle, which scales as $1/\sqrt{N}$.

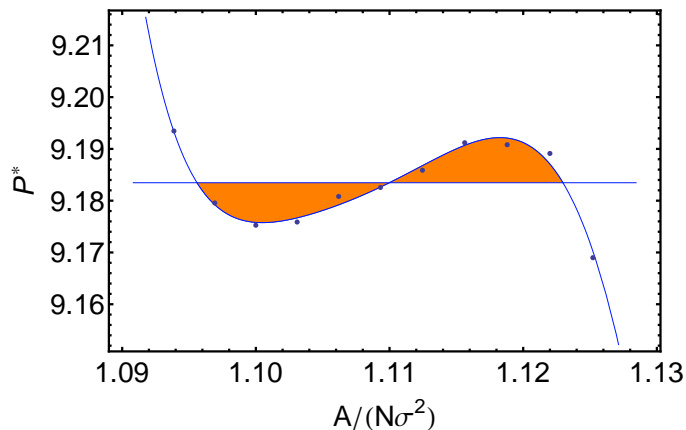


FIG. 2: Maxwell construction for $N = 1024^2$ hard spheres confined between two parallel hard walls for $H/\sigma = 1$. The reduced 2D lateral pressure $P^* = \beta P \sigma^2$ as a function of the area per particle $A/N\sigma^2$. The horizontal line denotes the bulk coexistence pressure $P_{co}^* = 9.183$. The blue curve is a 7th-order polynomial fit to the simulation data. The height of the horizontal line is such that the orange areas below and above the horizontal line are equal.

Maxwell constructions to obtain the coexisting densities, η_L and η_H , and the interface free energy per particle f (Fig. 3 and Table 1).

FINITE SIZE SCALING OF THE 2D POSITIONAL ORDER PARAMETER

In order to characterize the coexisting phase at high densities, we performed a sub-block scaling analysis to the 2D positional order parameter $\Psi_G = \left| \frac{1}{N} \sum_{i=1}^N \exp(i\mathbf{G} \cdot \mathbf{r}_i) \right|^2$ in reciprocal space, where the sum runs over all particles i , \mathbf{r}_i is the 2D projection of the position of particle i and \mathbf{G} denotes the wave vector that corresponds to a diffraction peak and equals $2\pi/a$ with a the averaged lattice spacing. We remark here that the average lattice spacing might differ from the lattice spacing of an ideal triangular lattice due to vacancies and other defects [1]. In addition, the crystal can rotate in the simulation box and thus the direction of \mathbf{G} can vary from $-\pi/3$ to $\pi/3$. In our calculations, we

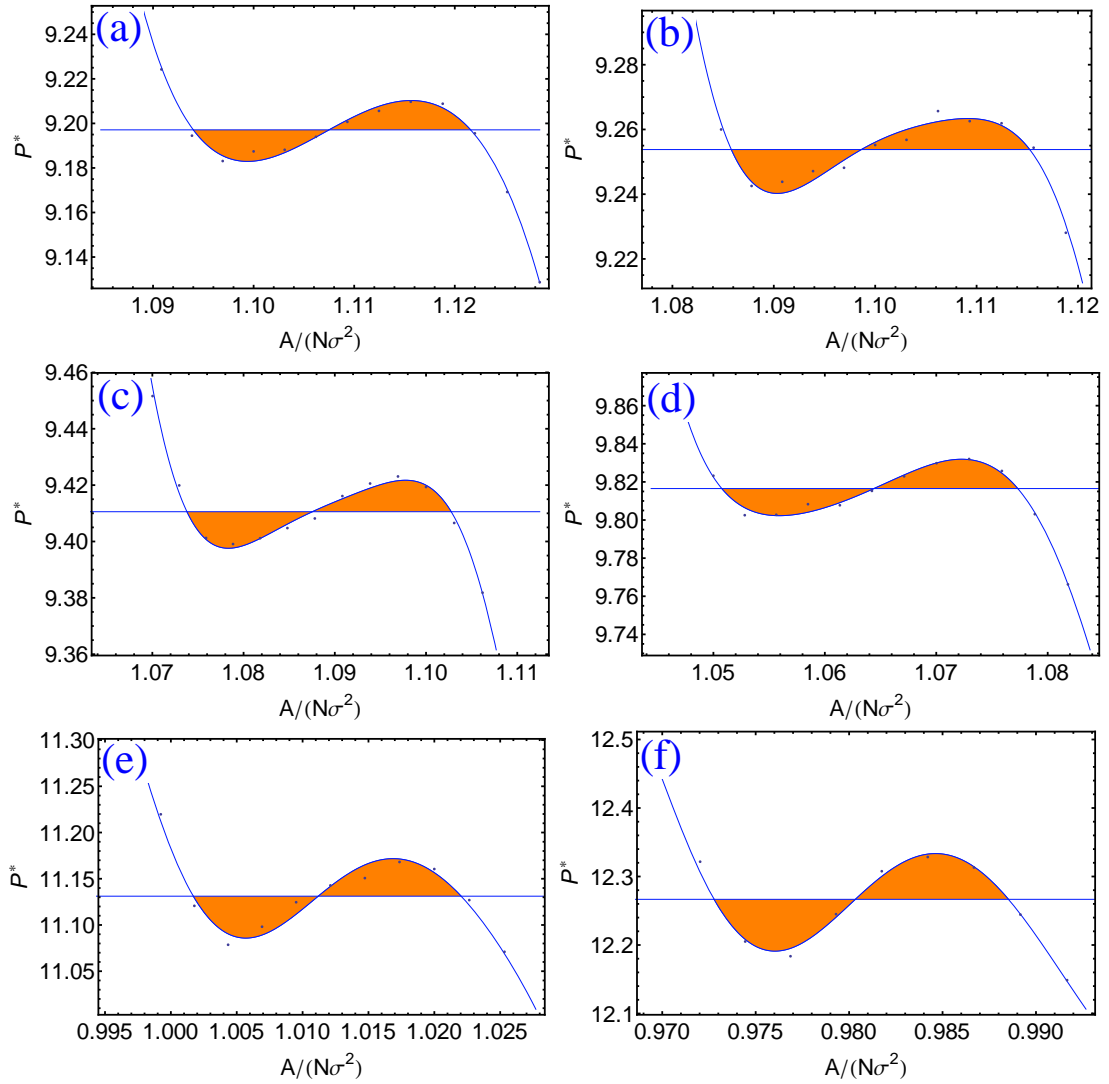


FIG. 3: Maxwell construction for $N = 1024^2$ hard spheres confined between two parallel walls. The reduced 2D lateral pressure $P^* = \beta P \sigma^2$ as a function of the area per particle $A/N\sigma^2$ for plate separation (a) $H/\sigma = 1.1$, (b) 1.2, (c) 1.3, (d) 1.4, (e) 1.5, and (f) 1.53. Blue curves are polynomial fits to the simulation data. Horizontal lines denote the Maxwell constructions, i.e., the orange areas above and below the horizontal line are equal.

employed the wave vector \mathbf{G} that yielded the maximal $\Psi_{\mathbf{G}}$. We calculated $\Psi_{\mathbf{G}}$ for varying sub-block sizes L_B/L with $L = \sqrt{L_x L_y}/4$ and analyzed the scaling of $\ln(\Psi_{\mathbf{G}}(L_b)/\Psi_{\mathbf{G}}(L))$ versus $\ln(L_b/L)$. According to the KTHNY theory, the finite-size scaling plot of the translational order is non-linear in the liquid and hexatic phase, whereas it is linear in the solid phase as the positional order parameter decays algebraically with an exponent $0 \leq \alpha \leq 1/3$. Fig. 4 shows the finite-size scaling analysis for $H/\sigma = 1.0, 1.2, 1.3, 1.4, 1.5$, and 1.53. For all plate separations $1 \leq H/\sigma \leq 1.53$, we find that the transition to the solid phase occurs at a higher density than the coexisting densities as determined from the Maxwell construction, indicating a first-order liquid-hexatic transition, and a small density regime with a stable hexatic phase.

CORRELATION FUNCTIONS OF THE POSITIONAL AND BOND-ORIENTATIONAL ORDER

We also computed the positional correlation function in reciprocal space $g_{\mathbf{G}}(r)$ and the bond orientational order correlation function $g_6(r)$. Fig. 5 shows the correlation functions of the positional order $g_{\mathbf{G}}(r)$ for $H/\sigma = 1.0, 1.2, 1.3$ and 1.4 at varying packing fractions η . The positional order decays exponentially in the liquid and hexatic phase. In the solid phase, the positional order decays with a power law $r^{-\alpha}$ with $\alpha = 1/3$ at the solid-hexatic transition according

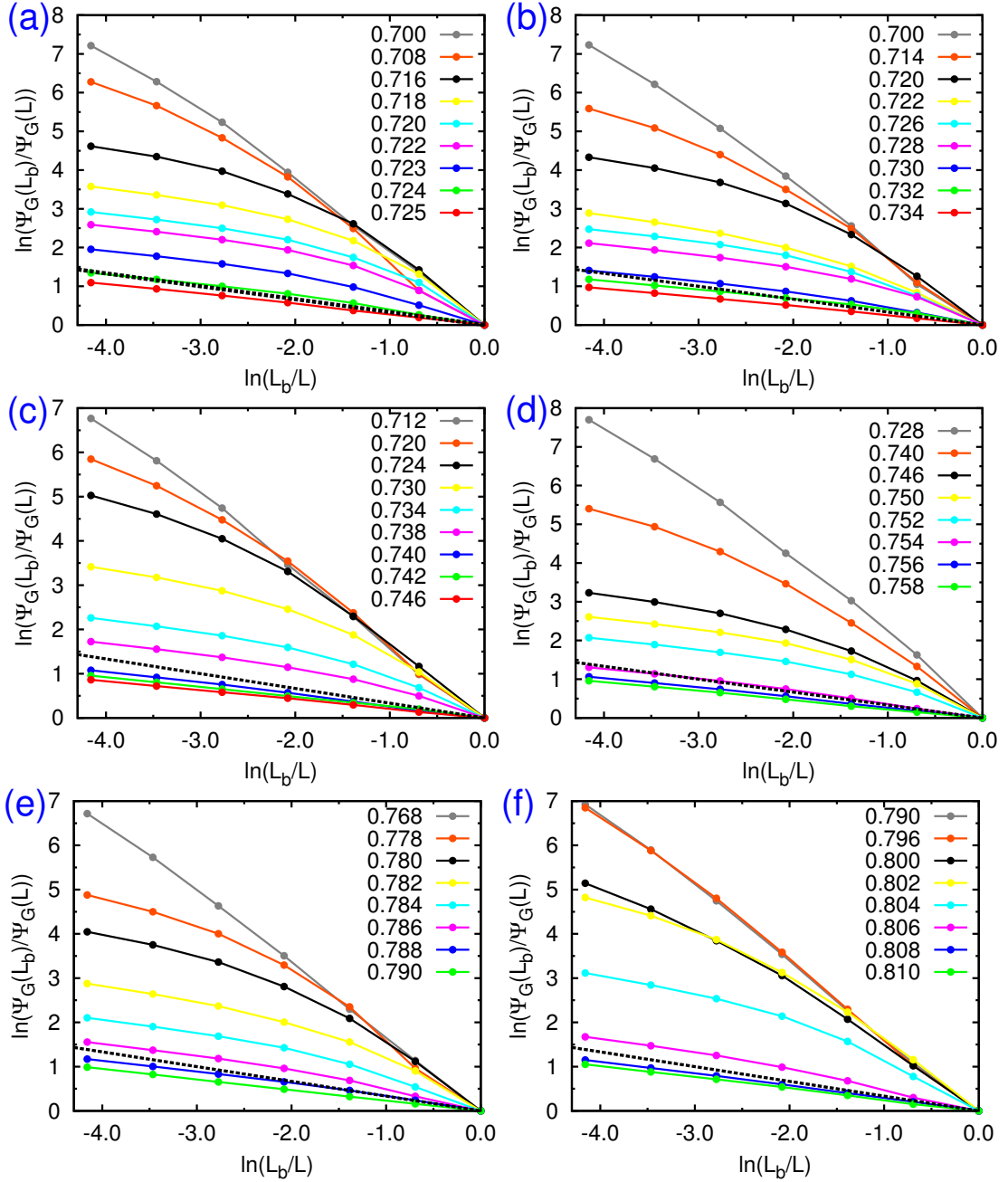


FIG. 4: Sub-block scaling analysis of the 2D positional order parameter in reciprocal space $\Psi_G(L_b)$ versus L_b for hard spheres confined between two plates with (a) $H/\sigma = 1.0$, (b) $H/\sigma = 1.2$, (c) $H/\sigma = 1.3$, (d) $H/\sigma = 1.4$, (e) $H/\sigma = 1.5$ and (f) $H/\sigma = 1.53$ and for varying η as labeled. The slope of the black dashed line is $-1/3$, which indicates the transition to the solid phase according to the KTHNY theory.

to the KTHNY theory. We find that the density at which the hexatic phase transforms into a solid phase is higher than the coexisting densities as obtained from the Maxwell constructions for all plate separation values considered, thereby confirming the presence of a stable hexatic phase. In addition, we find that the positional correlation function $g_G(r)$ is well-fitted by a stretched exponential function $e^{-(r/\xi)^\beta}$ in the hexatic phase with a correlation length $\xi \sim 20\sigma$ and $0.2 \leq \beta \leq 1$.

Fig. 6 shows the correlation function of the bond orientational order for $H/\sigma = 1.0, 1.2, 1.3$ and 1.4 for systems consisting of $N = 1024^2$ hard spheres confined between two parallel hard walls. In the liquid phase, the bond orientational order decays exponentially, whereas in the hexatic phase the orientational order decays with a power law $r^{-\alpha}$ with $\alpha = 1/4$ at the hexatic-liquid phase transition according to the KTHNY theory. The coexisting phase

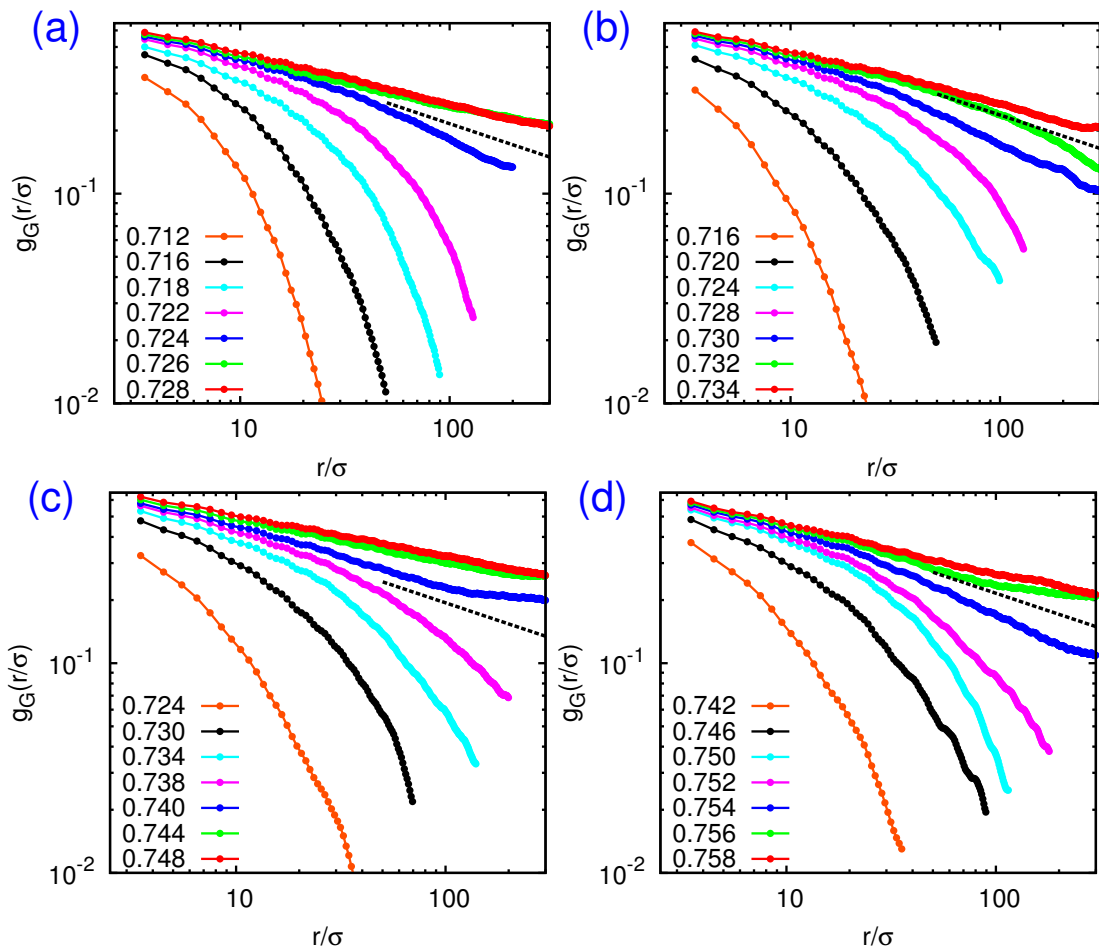


FIG. 5: Positional correlation function $g_G(r)$ as a function of r for hard spheres confined between two plates with (a) $H/\sigma = 1.0$, (b) $H/\sigma = 1.2$, (c) $H/\sigma = 1.3$ and (d) $H/\sigma = 1.4$ and varying η as labeled. The slope of the black dashed line is $-1/3$, which indicates the transition to the solid phase according to the KTHNY theory.

at high densities indeed show algebraic bond orientational order, confirming that the liquid coexists with an hexatic phase.

* Electronic address: M.Dijkstra@uu.nl

- [1] E. P. Bernard and W. Krauth, Phys. Rev. Lett. **107**, 155704 (2011).
- [2] M. Engel, J. A. Anderson, S. C. Glotzer, M. Isobe, E. P. Bernard, and W. Krauth, Phys. Rev. E **87**, 042134 (2013).
- [3] D. C. Rapaport, *The Art of Molecular Dynamics Simulation* (Cambridge University Press, 2004).
- [4] J. E. Mayer and W. W. Wood, J. Chem. Phys. **42**, 4268 (1965).

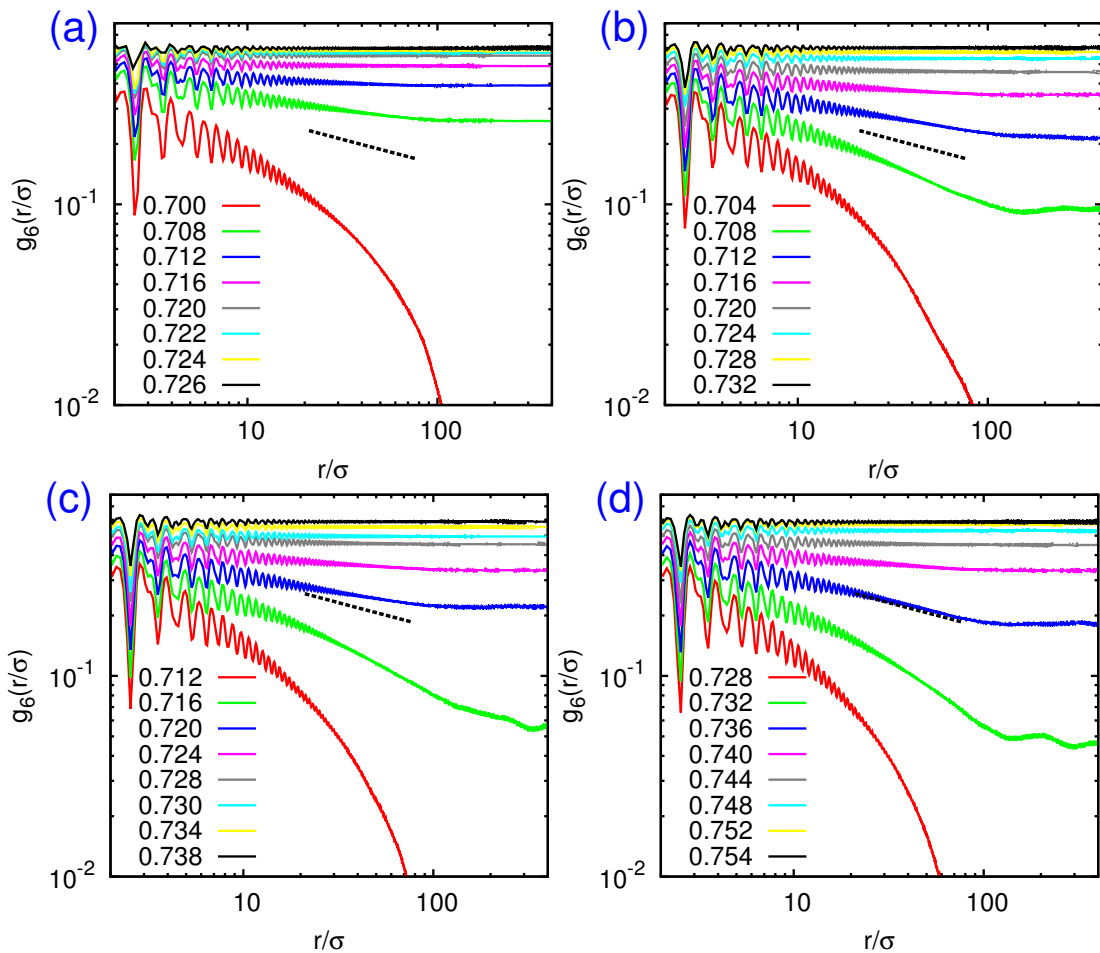


FIG. 6: Bond orientational order correlation function $g_6(r)$ as a function of r for hard spheres confined between two parallel hard plates with (a) $H/\sigma = 1.0$, (b) $H/\sigma = 1.2$, (c) $H/\sigma = 1.3$ and (d) $H/\sigma = 1.4$, and varying η as labeled. The slope of the black dashed line is $-1/4$, which indicates a hexatic-liquid transition according to KTHNY theory.